MD simulations of hydrogen diffusion in ZIF-11 with a force field fitted to experimental adsorption data

P. Schierz [a],[*], S. Fritzsche [a],[b], W. Janke [a], S. Hannongbua [b], O. Saengsawang [c], C. Chmelik [d], J. Kärger [d]

[a] Institute for Theoretical Physics, Faculty of Physics and Earth Science, University of Leipzig, Postfach 100 920, 04009 Leipzig, Germany
[b] Chulalongkorn University, Computational Chemistry Unit Cell (CCUC), Department of Chemistry, Faculty of Science, Bangkok 10330, Thailand
[c] Office of Corporate R&D, IRPC Public Company Limited, Rayong, Thailand
[d] Institute for Experimental Physics I, Faculty of Physics and Earth Science, University of Leipzig, Linnéstr. 5, 04103 Leipzig, Germany

ARTICLE INFO

ABSTRACT

Adsorption and diffusion of hydrogen in the metal organic framework ZIF-11 will be discussed in this paper using molecular dynamics (MD) and Gibbs Monte Carlo (GMC) computer simulations. Reliable force fields, needed for these simulations, are only partially available. Adsorption simulations, in comparison with experiments, have been used to fit some missing interaction parameters. The lattice flexibility turns out to have relatively small influence on adsorption. The obtained parameter set has been used to investigate the structure of ZIF-11 and the self-diffusion of hydrogen within the flexible framework.

© 2014 Elsevier Inc. All rights reserved.

1. Introduction

The properties of porous materials have become a topic of great interest for basic research as well as for practical applications. Two of the most common aims are to improve selectivity and storage properties for sorbent applications. In recent years, metal organic frameworks (MOFs) have become porous materials of great interest because of their promising properties and because of the big variety of structures that can be obtained from the combinations of metal knots and organic linkers [1]. ZIFs (zeolitic imidazolate frameworks), as one subgroup of MOFs, have attracted attention due to their exceptional chemical and thermal stability [2].

In [2] Park et al. have tested the ZIFs for their chemical and thermal stability. They have selected two porous structures with a high pore volume and small apertures as attractive subjects, namely ZIF-8 and ZIF-11. ZIF-11, in comparison with ZIF-8, has shown higher hydrogen uptake for low pressures, while both materials are comparable in their hydrogen uptake at standard pressure.

Additionally, ZIF-8 showed a slightly better performance regarding the thermal stability of the framework. This slightly better thermal stability might have been one of the reasons why ZIF-8 has become a popular research topic (see e.g. [3–8]) while there are only a few publications on simulation approaches to ZIF-11, so far (see e.g. [9]), such as this work.

Previous investigations of MOFs have shown that, for example, the framework shape and the flexibility of MOFs are crucial properties, notably influencing the dynamics of guest molecules. Several MOFs are much more flexible than, e.g., zeolites. This flexibility can strongly change the size and concentration dependence of the self-diffusion coefficient. This was shown, for example, by Seehamart et al. [10,11] for Zn(tbip) or by Hertäg et al. [3] and Zheng et al. [5] for ZIF-8. For ZIF-6 even a gate opening effect was proposed [12] that, most surprisingly, enabled the adsorption of molecules larger than the windows connecting adjacent pores. Passing the windows, however, is obviously the only way how molecules may migrate from pore to pore. The gate opening effect was confirmed to exist with N_2 in ZIF-8 [13], both by simulations with different structures and by experiment. This finding was confirmed in extensive MD simulations [14,15].

For simulating such a flexible framework it is also necessary to describe the interactions due to the chemical bonds of the lattice. Thornton et al. [9] have performed first simulations for a flexible ZIF-11 lattice for permeability and selectivity predictions. Unlike

* Corresponding author.
E-mail addresses: schierz@itp.uni-leipzig.de (P. Schierz), siegfried.fritzsche@uni-leipzig.de (S. Fritzsche), wolfhard.janke@itp.uni-leipzig.de (W. Janke), Supot.H@chula.ac.th (S. Hannongbua), oraphan.s@pttplc.com (O. Saengsawang), chmelik@physik.uni-leipzig.de (C. Chmelik), kaerger@physik.uni-leipzig.de (J. Kärger).

Thornton et al. we did not use the DREIDING force field for the parameters of the bonded forces, since DREIDING was found to be too stiff in simulations for diffusion of methane in ZIF-8 [3]. This was decisive for this system, where the size of the guest molecules is slightly larger than the window diameter. For the small hydrogen molecules in ZIF-11, however, this influence has to be much smaller and will most likely reduce the effects of a stiffer force field. We anticipate, therefore, that the results of Thornton et al. [9] and this work should be at least of the same order of magnitude.

For this work we developed and tested a flexible force field for ZIF-11 without partial charges. The parameter values were fitted and adapted to yield a good agreement with both the adsorption isotherm from Park et al. [2] and the X-ray structure from the Cambridge structural data base [16].

2. X-ray structure

The X-ray structure of ZIF-11 was provided by the Cambridge Crystallographic Data Centre [16] as determined by Park et al. [2]. As a special property of the X-ray structure multiple configurations are possible for most of the linkers. This experimental X-ray structure has been investigated to construct a reasonable choice for the atom configurations in the simulation box. This choice, especially of the linkers which are forming the connections of adjacent cavities, turned out to be crucial for the diffusion behavior.

As a starting point of our considerations, the linker configurations were specifically chosen in order to avoid unreasonably strong repulsion of neighboring linkers. For some of the linkers there was a choice between a flat or bended configuration. Having chosen all the linkers as flat would have led to a strong Lennard-Jones repulsion force in the configuration state of the measured X-ray structure. The same result was obtained when all linkers were bent. Therefore it was necessary to carefully combine the linker positions in an alternating way to get a reasonable total configuration. Another line of reasoning has been followed in the choice of the linkers forming the connections between adjacent cavities. Some possible combinations of linker configurations were ruled
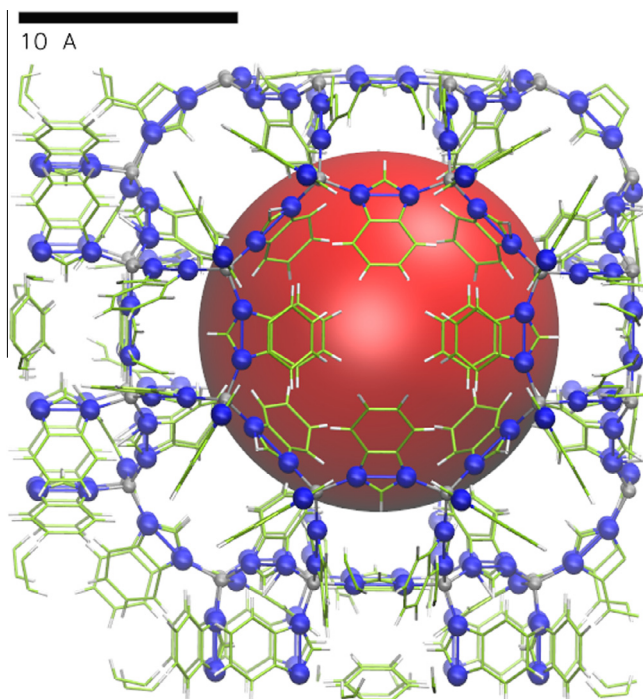

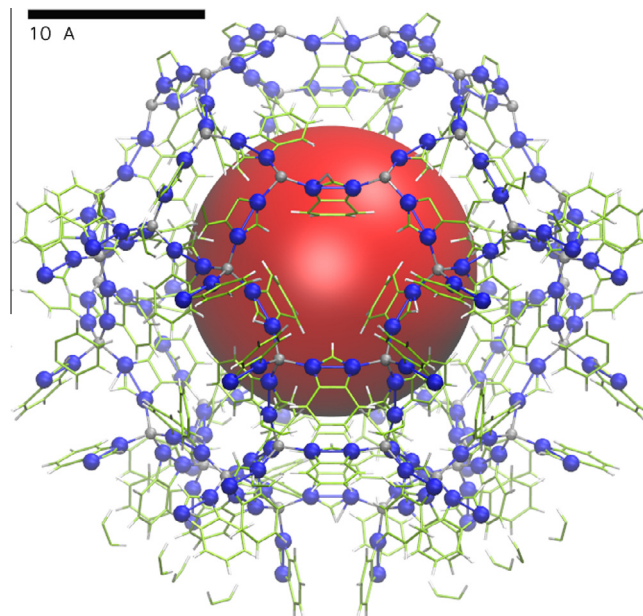**Fig. 1.** ZIF-11 structure viewed through the 8-membered ring.

Fig. 2. ZIF-11 structure viewed through the 6-membered ring window.

Table 1
Table of mean deviation of the average atom positions from the X-ray structure.

Example	Mean deviation from the X-ray structure per particle in Å
MD simulation including charges	0.315122
MD simulation excluding charges	0.06133

out based on the previously mentioned reasoning. Two remaining possibilities were tested in simulations. In these simulations, one of these two configurations was found to completely prohibit any hydrogen diffusion and was therefore ruled out. The choice of the linker configurations is explained in further detail in the supplementary material. Two snapshots of the positions of the lattice atoms as chosen for our simulations are shown in Figs. 1 and 2.

It was important to describe the different linker types with different parameters. In this way it was possible to reproduce the crystal structure up to a high accuracy (see Table 1) and to guarantee that the shape of the windows corresponds to the shape determined by X-ray diffraction.

3. Force field development

The parameter set needed for a complete description of the force field has to take account of non-bonded and bonded interactions. We describe the potential energy for the ZIF-11 lattice with a 12–6 Lennard-Jones potential for the non-bonded interaction and harmonic bond, valence angle and dihedral angle interactions representing the interactions due to the chemical bonds of the lattice, yielding:

$$E = \sum_{i=1}^{N}\sum_{j>i}^{N} 4\epsilon_{ij}\left[\left(\frac{\sigma_{ij}}{r_{ij}}\right)^{12} - \left(\frac{\sigma_{ij}}{r_{ij}}\right)^{6}\right] + \sum_{m_{\text{bond}}(i,j)}^{N_{\text{bond}}}\frac{1}{2}\alpha_m(r_{ij}-r_m)^2$$

$$+ \sum_{n_{\text{angle}}(i,j,k)}^{N_{\text{angle}}}\frac{1}{2}\beta_n(\phi_{ijk}-\phi_n)^2 + \sum_{o_{\text{torsion}}(i,j,k,l)}^{N_{\text{torsion}}}\gamma_o\left[1+\cos(p_o\theta_{i,j,k,l}-\theta_o)\right].$$

(1)

3.1. Lennard-Jones parameters

The Lennard-Jones parameters for the lattice interactions were taken from AMBER [17]. The Lorentz-Berthelot mixing rules were applied to get the Lennard-Jones parameters $\sigma_{ij}, \epsilon_{ij}$ between atoms of different type. To avoid incompatibilities it was attempted to take, if possible, all parameters from one source, namely the AMBER force fields. Unfortunately, in AMBER such parameters were not available for the hydrogen–hydrogen interaction.

The hydrogen molecules were also treated as Lennard-Jones particles. This is reasonable since the H_2-H_2 interactions are very weak and hydrogen molecules are rotating very fast [18,19]. The values for the Lennard-Jones interaction parameters are varying in the literature (see Table 4). This reflects the difficulty to satisfactorily represent the behavior of different systems over a wide temperature range with only one parameter set. In our studies we adjusted the hydrogen Lennard-Jones parameters to fit the measured adsorption isotherm of ZIF-11 by Park et al. [2].

We had to decide to either follow the common approximation used by many authors for simulating adsorption in a rigid ZIF lattice (see, e.g., the review by Krishna et al. [20] and the literature cited there or Babarao et al. [21] and their statement about the rigid lattice and the literature cited there) or to also perform the computer-time expensive fitting part of our work with a flexible lattice. Exceptional systems, where the rigid lattice approximation would not be possible, would be ZIFs that show a phase transition at higher loading for some kinds of guest molecules that leads, e.g., to inflections in the adsorption isotherm or to 'gate opening' [12,14,15]. This is not the case for hydrogen in ZIF-11. Our decision was to fit missing parameters by Gibbs Monte Carlo simulations using the rigid lattice and to check this approximation afterwards. Comparing the results of MD simulations for the adsorption isotherm using, respectively, rigid and flexible lattices we did in fact obtain satisfactory agreement.

Fig. 3 moreover illustrates that it was possible to get also good agreement with the experimental adsorption isotherm by only varying the hydrogen–hydrogen interaction parameters. The resulting Lennard-Jones parameters of the hydrogen interaction were $\epsilon_{H_2} = 0.314 \frac{kJ}{mol}, \sigma_{H_2} = 2.88$ Å (see Table 4). The adsorption data were reproduced more accurately than in a previous paper [9]. So far we could not find additional data to validate the H_2-H_2 force field under additional pressure and temperature conditions.
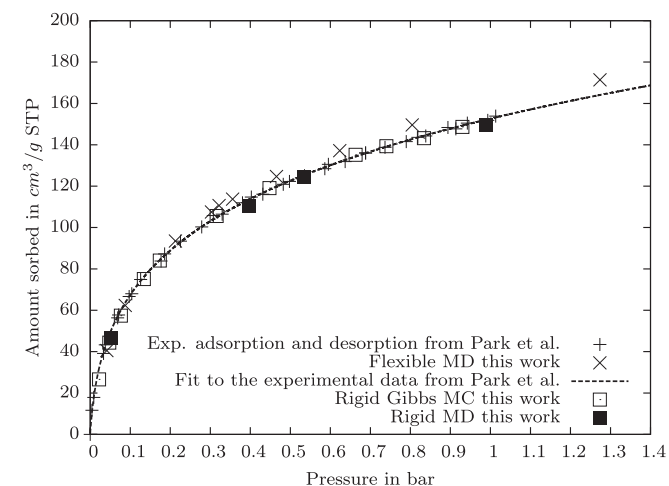
3.2. Bonded interactions

The parameters for the bonded interactions were divided into two groups, namely those which define distances and angles (r_m, ϕ_n and θ_o), which will be referred to as geometrical parameters, and the remaining ones: ($\alpha_m, \beta_n, \gamma_o$ and p_o) which will be referred to as non-geometrical parameters.

The geometrical parameters were directly computed from the X-ray structure as the real bond lengths, valence angles and dihedral angles. The non-geometrical parameters of the organic linkers were taken from AMBER. The harmonic bond interaction for the Zn-N bond, the valence angle interactions of N-Zn-N, CK-N-Zn and CB-N-Zn were taken from the paper of Zheng et al. [5] for ZIF-8 since the configurations for these bonds in ZIF-11 are very similar to the corresponding ones in ZIF-8. In [5] the dihedral interaction of X-Zn-N-X was completely neglected to guarantee a high mobility of the linkers. Since it was not mentioned in more detail why this torsion potential should be completely neglected, a value for this interaction was taken from the paper of Ryde [22] as described in the supplementary material. The value of γ_o (see Eq. (1)) for this dihedral interaction potential was small in comparison with the other torsion interaction parameters γ_o.

The force field of this work neglects partial charges of the lattice for several reasons. Since hydrogen is treated as a neutral Lennard-Jones particle, partial charges of the lattice would directly influence only the lattice-lattice interaction but not the lattice-hydrogen interaction. The influence of partial charges was tested in a flexible MD simulation without guest molecules, using a set of charges calculated with the GAUSSIAN software and the module "antechamber" [23] of AMBER. In these tests we found that the introduction of our partial charges leads to unacceptable lattice deformations (see Table 1). Moreover, by the introduction of partial charges additional connections of adjacent cavities were created which were in disagreement with the X-ray structure. They are shown in equipotential plots (see supplementary material for definition) calculated from the average lattice atom positions of an MD simulation including charges (see Figs. 4 and 5).
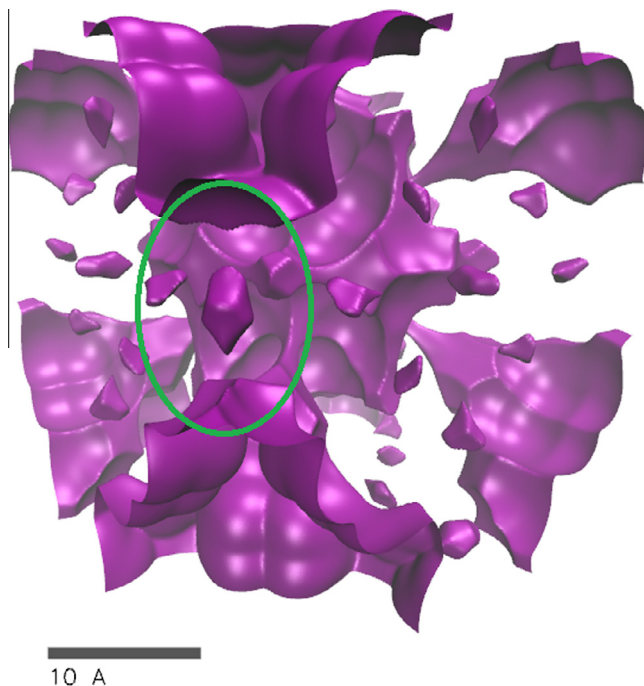

Fig. 3. Adsorption isotherm for hydrogen in ZIF-11 at 77 K in comparison with the results of Park et al. [2]. The unit $\frac{cm^3}{g}$ STP means the amount of volume that the guest particles in one gram of MOF material would occupy, at standard pressure and temperature, according to the ideal gas equation. For ZIF-11 the y-axis can be multiplied with 0.64 to get the number of guest particles per unit cell.

Fig. 4. ISO surface plot at 3 kJ/mol calculated from the average atom positions of a NVE simulation excluding charges.
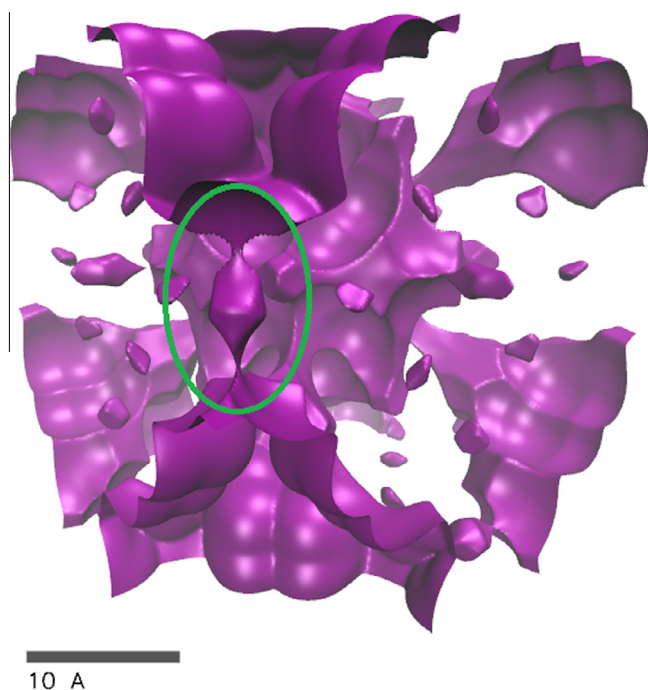
Fig. 5. Same as Fig. 4, but with charges taken into account.

Additionally, short NPT test simulations (where we used a barostat in the DL_Poly software package [24]) at 1 bar revealed that the lattice constant (simulation box size) was shrinking considerably in the MD simulation with charges while there is a deviation of only 1.1 % in the MD simulation without charges (see Table 2).

Since it was the aim of the present paper to get a reliable force field for hydrogen self-diffusion, partial charges have been neglected to avoid unreasonable deformations of the lattice framework. It is desirable to improve this parameter set in the future to obtain a force field that can also be used for charged particles. In [25] a way is proposed to do that. The basic idea is that the resulting force field should create a stationary state with zero acting force when it is applied to the measured X-ray configuration. If the reasonable assumption holds that this stationary configuration is close to the average configuration of the vibrating lattice the force field would reproduce the X-ray configuration in a good manner. Therefore the force field without charges would have to be adapted to compensate for the acting electrostatic forces in the X-ray configuration to get again a stationary state for the X-ray configuration.

An alternative way based on the use of modified Amber parameters in ZIF-11, including charges, is described in [26]. But we will not refer to it in greater detail since we are concerned with the diffusion and adsorption of the neutral H_2 for which our model with uncharged particles is sufficient.

The here proposed lattice force field is an effective one for neutral guest molecules. The development of such a force field for neutral guest molecules makes sense not only because of the

Table 2
Table of the stable box lengths.

Example	Stable box length in Å
MD simulation including charges	26.56
MD simulation excluding charges	28.44
X-ray structure	28.76

problems with lattice stability described above. Charges would, additionally, require Ewald summation or equivalent techniques that makes simulations much more computer-time expensive. This effort can be avoided for the study of neutral guest molecules in ZIF-11.

The complete table of the interaction parameters, used in this work can be found in the supplementary material.

4. Simulation details

The DL_Poly software package [24] was used to carry out the MD simulations for hydrogen in ZIF-11. The simulations, which were carried out with periodic boundary conditions, have been restricted to one unit cell of ZIF-11 to keep the computational effort at a reasonable level. The cutoff was chosen as 13 Å which means, for the biggest Lennard-Jones particles, a cutoff of 3.8σ. It was ensured that the cutoff is still smaller than half of the simulation box length (14.38 Å). The simulations have been done in the NVE ensemble with the Velocity-Verlet integrator. In the thermalization period the system relaxed into a state in which, over short periods, the average kinetic energy was corresponding to the aspired average temperature. In the long NVE runs, the total temperature average agreed quite well with this value. The simulations were carried out with a time step of 1 fs. Depending on the statistics for the self-diffusion coefficient, 20–60 ns runs have been performed. For bonded atoms and for valence angle interacting atoms the non-bonded Lennard-Jones interaction was neglected. For the dihedral interaction the non-bonded Lennard-Jones interaction was scaled by a factor of 0.5. This convention is widely used (see e.g. [5]) and avoids an overlap of bonded interaction potentials and van der Waals (VDW) potentials. These potentials even differ in the points of their minima which would result in a distortion of the lattice structure.

5. Results

5.1. Connectivity of the ZIF-11 structure for hydrogen

The investigation of the X-ray structure with equipotential plots revealed that there are two types of pores in the unit cell of ZIF-11. Only different pore types are connected while, at room temperature, there is no connection between pores of the same type (see Fig. 6). This conclusion has been made by comparing the mean kinetic energy at a certain temperature with the height of the potential walls in possible connections between adjacent cavities. Particle diffusion necessitates an uninterrupted path between adjacent pores which, obviously, is only the case with kinetic energies of at least the order of magnitude of barriers in the potential energy along this path. For further explanation we refer to the supplementary material.

Kortunov et al. [27] mentioned the possibility that 8-ring and 6-ring apertures exist in ZIF-11. The present investigation revealed that there is only one type of connection of adjacent cavities at standard ambient temperature and for the here developed force field. This connection is the 6-ring window of the structure.

5.2. Adsorption isotherm

The hydrogen–hydrogen Lennard-Jones interaction parameters were fitted by rigid Gibbs Monte Carlo simulations to get good agreement with the measured adsorption isotherm. To explore the influence of lattice flexibility on adsorption we used the Widom test particle method to estimate the chemical potential in flexible MD simulation. The pressure in the gas phase surrounding the porous material can be estimated on the basis of the
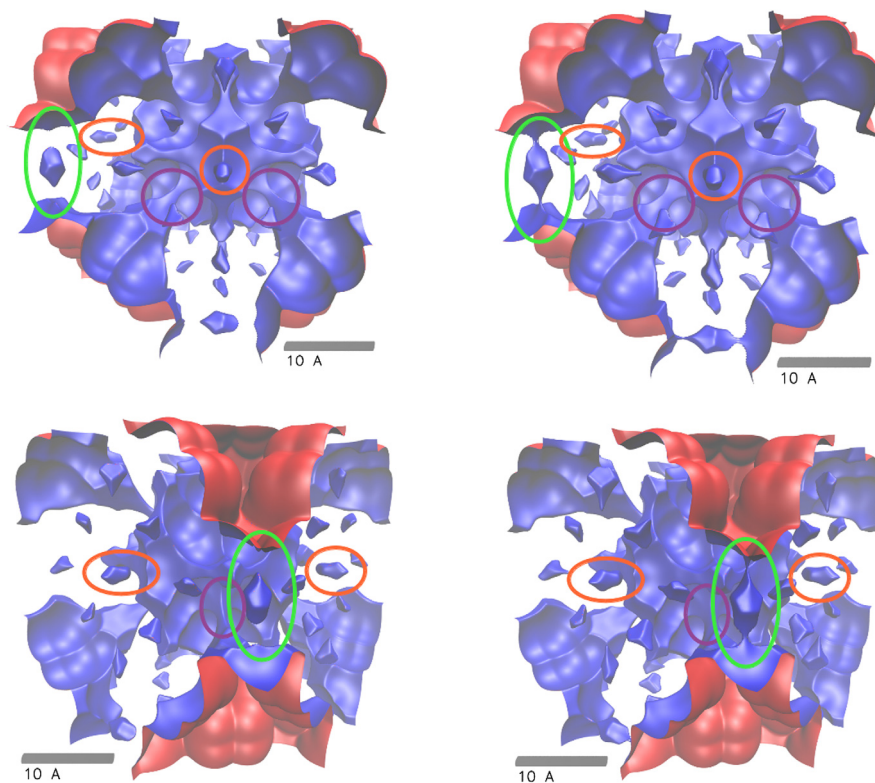
(a) Isopotential surface of ZIF-11 at $3\frac{\text{kJ}}{\text{mol}}$ with markers for the possible connections between adjacent cavities which are opened (purple) or closed (green and orange) [25].

(b) Isopotential surface of ZIF-11 at $12\frac{\text{kJ}}{\text{mol}}$ with markers for the possible connections between adjacent cavities which are opened (purple, green) or closed (orange) [25].

Fig. 6. The isopotential surface of ZIF-11 at (a) $3\frac{\text{kJ}}{\text{mol}}$ and (b) $12\frac{\text{kJ}}{\text{mol}}$. The lower plots show a different view, rotated by roughly 45° around the z-axes. The blue isopotential surface (colored in the web version) is encapsulating the pores of the ZIF-11 structure. The red surface is also an isopotential surface at a slightly lower energy to differentiate between outer and inner surface of pores. A connection between the two surfaces, which are surrounding the pores, stands for a potential energy barrier lower than the isopotential value ($3\frac{\text{kJ}}{\text{mol}}$ and $12\frac{\text{kJ}}{\text{mol}}$ respectively). In (a) only the path marked in purple is connected while in (b) there is also an connection between the isosurfaces marked with green ellipses. The other ellipses are around low energy bubbles which are disconnected from the pores by high-energy regions. (For interpretation of the references to colour in this figure legend, the reader is referred to the web version of this article.)

calculated chemical potential and the given temperature, since the chemical potential of the gas molecules in the adsorbed phase and the surrounding atmosphere have to coincide. Under the conditions considered in this paper, hydrogen in the surrounding atmosphere can be treated as an ideal gas (for further argumentation see the supplementary material). Therefore, the ideal gas relation was used to determine the pressure of the surrounding gas from the measured chemical potential and temperature.

For comparing the two calculation methods (molecular dynamics and Gibbs Monte Carlo simulations) rigid MD simulations were performed. They turned out to be in good agreement with the rigid Gibbs MC simulations, as expected. Fig. 3 shows the results of those simulations. The pressure in flexible MD simulations was slightly higher than in the rigid Gibbs MC simulations. This shows a (slight) influence of the flexible lattice for MOFs, even on adsorption properties. But, this influence of the flexibility on the amount of adsorbed hydrogen is much less prominent than the influence of the lattice flexibility on diffusion, where the fluctuating size of the window is more important and would be even crucial for larger molecules [3].

5.3. Self-diffusion coefficient

The obtained force field was used to calculate values for the self-diffusion coefficient for various temperatures and loadings.

The self-diffusion coefficient was calculated from MD simulations with the Einstein relation [28,29]:

$$D_{\text{self}} = \lim_{t \to \infty} \frac{\text{d}}{\text{d}t} \sum_{i=1}^{N} \frac{\langle (\mathbf{r}_i(t + t_0) - \mathbf{r}_i(t_0))^2 \rangle}{6N}. \tag{2}$$

Here $\mathbf{r}_i(t + t_0)$ and $\mathbf{r}_i(t_0)$ means the coordinates of guest particle i at time t and t_0, respectively, N is the total number of guest molecules and $\langle \ldots \rangle$ denotes the ensemble average.

Two dependencies of the self-diffusion coefficient were investigated: the temperature dependency and the loading dependency. The temperature dependency of the self-diffusion coefficient for porous materials can often be described with the Arrhenius law [28,29]:

$$D_{\text{self}}(T) = D_0 \cdot \exp\left(-\frac{E_A}{k_B T}\right), \tag{3}$$

where E_A is the activation energy. To test whether this relation is applicable for ZIF-11, different simulations for the same loading of 5 molecules per unit cell and different temperatures were performed. The resulting self-diffusion coefficients have been in good agreement with the Arrhenius law as can be seen in Fig. 7. The parameters in (3) obtained from a least square fit are $E_A = 3.724 \pm 0.16 \frac{\text{kJ}}{\text{mol}}$ and $D_0 = (3.59 \pm 0.44) \times 10^{-8} \frac{\text{m}^2}{\text{s}}$. The error bars were calculated from the linear fit. It has to be noted that this can only be

seen as an approximate estimation of the temperature behavior since it is not well known in which temperature range the fitted force-field parameters are reliable.

We additionally tested, for one of the loadings, the influence of the flexibility upon the self-diffusion coefficient. At 77 K and a loading of 96 particles per unit cell we obtained a self-diffusion of $D_{self} = 3.02 \times 10^{-10} \frac{m^2}{s}$ in the flexible case and of $D_{self} = 5.56 \times 10^{-10} \frac{m^2}{s}$ in the rigid case.

A further simulation was performed with 5 particles per unit cell at 298 K. This condition corresponds to a pressure of 14 bar and is therefore comparable to the simulation conditions of Thornton et al. [9] who have performed simulations for 10 bar and 298 K. The resulting diffusion coefficients are in the same order of magnitude as can be seen in Table 3.

The second investigation was concerned with the loading dependence of the self-diffusion coefficient (Fig. 8). MD simulations for different loadings from 26 up to 120 particles per unit cell were performed. To estimate the error of the diffusion coefficient three test simulations with 80 particles per unit cell and different starting configurations have been performed. The thus estimated error was of the order of $\pm 0.3 \times 10^{-10} \frac{m^2}{s}$ at 77 K.

Even with this strong scattering, caused by statistical errors, the self-diffusion coefficient is seen to increase up to a loading of around 70–80 particles per unit cell (0.3–0.5 bar) and to decrease afterwards. Among the different patterns of loading dependence [30], hydrogen in ZIF-11 is thus seen to follow the type IV dependence. The decrease in the self-diffusion coefficient at very high loadings is clearly a consequence of the mutual hindrance of the molecules.

The diffusivity increase with concentration at low loadings can be explained by the influence of strong adsorption sites in the ZIF-11 lattice. The rapid change in the slope of the adsorption isotherm (see Fig. 3) for low pressures already indicates a rapid occupation of adsorption sites. A region of linear slope (Henry law region) cannot be identified. Another indication of such adsorption sites is provided by the radial distribution functions (see Fig. 9) between those lattice atoms which are forming the borders of adsorption sites and the guest molecules. Our results indicate an increased probability for lattice-guest contact. Additionally, these adsorption sites are displayed in Fig. 10 by a point cloud. This point cloud shows the guest particle positions accumulated after discrete time intervals during one simulation run. Therefore it is possible to highlight regions with a high probability of guest molecule
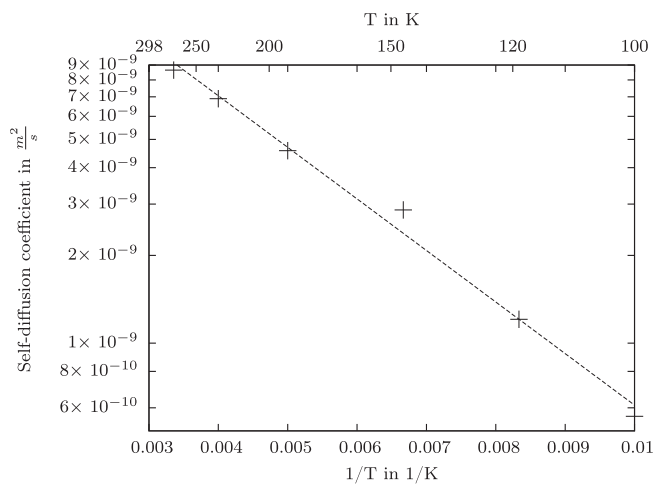
Table 3
Table of self-diffusion coefficients.

Simulation	Self-diffusion coefficient D_{self} in $10^{-9} \frac{m^2}{s}$
Thornton et al. [9]	7.2
This work	8.7

Table 4
Table of hydrogen interaction parameters.

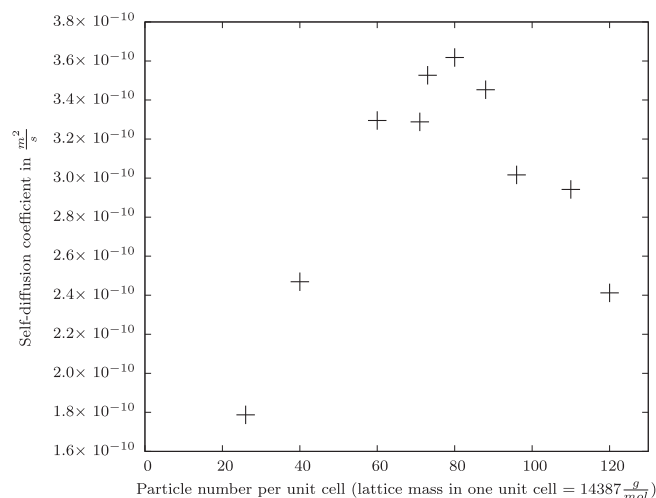| Source	Epsilon in $\frac{kJ}{mol}$	Sigma in Å
Knaap et al. [32]	0.308	2.928
Cheng et al. [33]	0.141	2.65
Darkrim et al. [34]	0.305	2.958
Rzepka et al. [35]	0.277	2.97
This work	0.314	2.88

Fig. 8. Loading dependence of the self-diffusion coefficient at 77 K.
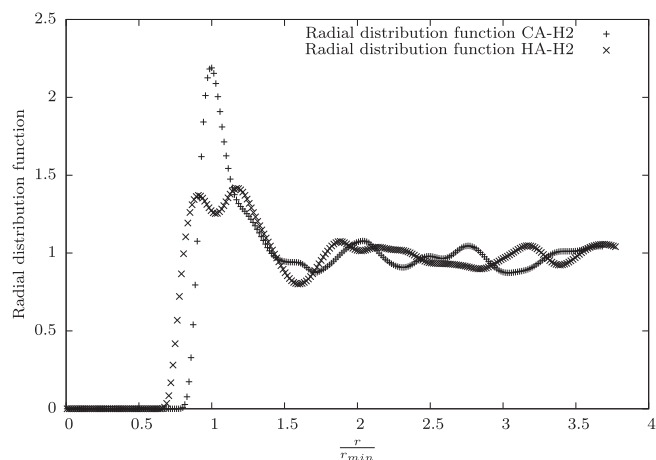

Fig. 9. Radial distribution functions measured between lattice atoms of type CA and HA and the guest molecules. For clarification of the atom types consult the supplementary material.

Fig. 7. Temperature dependence of the self-diffusion coefficient, together with a linear fit of $\ln(D_{self})$ versus $1/T$ according to the Arrhenius law (3) for a constant loading of 5 particles per unit cell.

occurrence. Additionally the figure shows an isopotential surface encapsulating the dense parts of the point clouds. Therefore it becomes obvious that the dense parts of the point clouds coincide with the potential minima.
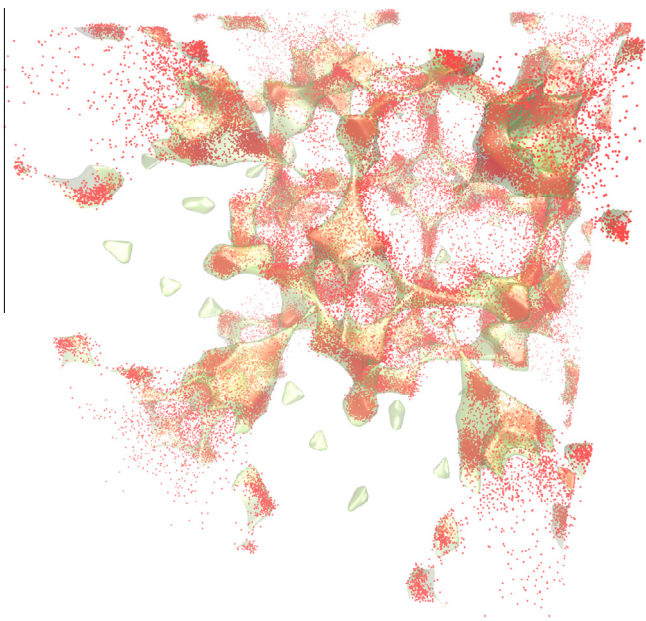
Fig. 10. Isopotential surface at $-4.53\frac{kJ}{mol}$ and a point cloud representing the probability density of the guest positions.

From time to time the guest molecules are trapped by strong adsorption sites. When many adsorption sites are already occupied by other guest molecules then the remaining guest molecules will have a longer average free path before they are trapped again at such an adsorption site. The same effect has been observed, e.g., by Chanajaree et al. for water in Chabazite [31].

6. Conclusions

The crystallographic structure of ZIF-11 was investigated with the conclusion that different linkers should be described with different MD parameters to reproduce the structure as it was determined by X-ray diffraction. It turned out that in ZIF-11, up to room temperature, there is essentially only one type of connections between adjacent cavities. The crystallographic structure of ZIF-11 was reproduced with a high accuracy and the lattice parameters (physical dimension of the unit cell) were shown to be reproduced in NPT test simulations. The force field presented in this work leads to good agreement with the complete experimental adsorption isotherm of hydrogen in ZIF-11, by fitting only the hydrogen–hydrogen Lennard-Jones parameters. For this type of material it is therefore possible to describe experimental values with the used type of force field for at least one temperature. This is encouraging since the used types of force fields are, in some cases, rather simple. The flexibility of the lattice had a small, but noticeable, influence on the adsorption data. To get full accuracy it is advisable to take account of the lattice flexibility of ZIF-11. The good agreement obtained between the simulated and measured adsorption properties is referred to the high accuracy of the ZIF-11 structure ensured in our simulations.

It would be most desirable to get further experimental data describing the lattice dynamics of ZIF-11 at 77K. The interaction parameters determining the dynamics were collected from the literature where they were applied to similar molecules. They could, however, not be compared with experiments.

The obtained force field has been used for the investigation of diffusion. The obtained results are expected to be rough estimates for real diffusion values since the force field is able to reproduce

the experimental data available so far. The calculated self-diffusion coefficient turned out to be in the same order of magnitude as the values reported by Thornton et al. [9].

The self-diffusivity was, moreover, simulated under varying conditions and will, hopefully, stimulate further experimental work for confirmation or dismissal.

Appendix A. Supplementary data

Supplementary data associated with this article can be found, in the online version, at http://dx.doi.org/10.1016/j.micromeso.2014.10.031.

References

[1] L. James, Chem. Soc. Rev. 32 (2003) 276.
[2] K.S. Park, Z. Ni, A.P. Cote, et al., PNAS 103 (2006) 10186.
[3] L. Hertäg, H. Bux, J. Caro, et al., J. Membr. Sci. 377 (2011) 36.
[4] Z. Hu, Y. Chen, Z. Jiang, J. Chem. Phys. 134 (2011) 134705.
[5] B. Zheng, M. Sant, P. Demontis, G.B. Suffritti, J. Phys. Chem. C. 116 (2012) 933.
[6] C. Zhang, R.P. Lively, K. Zhang, et al., J. Phys. Chem. Lett. 3 (2012) 2130.
[7] Z. Hu, L. Zhang, J. Jiang, J. Chem. Phys. 136 (2012) 244703.
[8] D. Fairen-Jimenez, R. Galvelis, A. Torrisi, et al., Dalton Trans. (2012), http://dx.doi.org/10.1039/c2dt30774j.
[9] A.W. Thornton, D. Dubbeldam, M.S. Liu, et al., Energy Environ. Sci. 5 (2012) 7637.
[10] K. Seehamart, T. Nanok, J. Kärger, et al., diusion-fundamentals.org 11 (2009) 38:1.
[11] K. Seehamart, T. Nanok, J. Kärger, et al., Microporous Mesoporous Mater. 130 (2010) 92.
[12] J. van den Bergh, C. Gücüyener, E.A. Pidko, et al., Chem. Eur. J. 17 (2011) 8832.
[13] D. Fairen-Jimenez, S.A. Moggach, M.T. Wharmby, et al., J. Am. Chem. Soc. 133 (2011) 8900.
[14] L. Zhang, Z. Hu, J. Jiang, JACS 135 (2013) 3722.
[15] T. Chokbunpiam, R. Chanajaree, T. Remsungnen, et al., Microporous Mesoporous Mater. 187 (2014) 1.
[16] F.H. Allen, Acta Crystallogr. Sect. B 58 (2002) 380.
[17] Y. Duan, C. Wu, S. Chowdhury, et al., J. Comp. Chem. 24 (2003) 1999.
[18] A.G. Donchev, N.G. Galkin, V.I. Tarasov, J. Phys. Chem. 126 (2007) 174307.
[19] F. Grazzi, M. Santoro, M. Moraldi, L. Ulivi, Chem. Eng. J. 85 (2002) 7.
[20] R. Krishna, J. van Baten, J. Phys. Chem. C 116 (2013) 23556.
[21] R. Babarao, S. Dai, D. Jiang, J. Phys. Chem. C 115 (2011) 8126.
[22] U. Ryde, Funct. Bioinfor. 21 (1995) 40.
[23] J. Wang, W. Wang, P.A. Kollman, D.A. Case, J. Mol. Graphics Modell. 25 (2006) 247.
[24] I.T. Todorov, W. Smith, K. Trachenkob, M.T. Doveb, J. Mater. Chem. 16 (2006) 1911.
[25] P. Schierz, Master Thesis, Universität Leipzig, unpublished (2012).
[26] W. Wongsinlatam, T. Remsungnen, Hindawi Publishing Corporation Journal of Chemistry, http://dx.doi.org/10.1155/2013/415027 2013 (2013) 000.
[27] P. Kortunov, Z. Ni, C. Paur, S. Reyes, J. Zengel, AIP Conf. Proc. 1330 (2011) 57.
[28] M.P. Allen, D.J. Tildesley (Eds), Computer Simulation in Chemical Physics, Dortrecht, Boston, London, 1993, Kluwer Academic Publishers, Proceedings of the NATO Advanced Study Institute on New Perspectives in Computer Simulation in Chemical Physics, Alghero, Sardinia, Italy, September 14–24, 1992.
[29] R. Haberlandt, S. Fritzsche, G. Peinel, K. Heinzinger, Molekulardynamik - Grundlagen und Anwendungen, mit einem Kapitel über Monte-Carlo-Simulationen von H. - L. Vörtler, Vieweg–Verlag, Wiesbaden, 1995.
[30] J. Kärger, D.M. Ruthven, D.N. Theodorou, Diffus. Nanoporous Mater., Wiley-VCH, Weinheim, 2012.
[31] R. Chanajaree, P. Bopp, S. Fritzsche, J. Kärger, Microporous Mesoporous Mater. 146 (2011) 106.
[32] H.F.P. Knaap, J.J.M. Beenakker, Physica 27 (1961) 523.
[33] H. Cheng, A.C. Cooper, G.P. Pez, et al., J. Phys. Chem. B 109 (2005) 3780.
[34] F. Darkrim, D. Levesque, J. Chem. Phys. 109 (1998).
[35] M. Rzepka, P. Lamp, M.A. De la Casa-Lillo, J. Phys. Chem. B 102 (1998) 10894.